Analysis of the Effect of Potential-Induced Degradation in Commercial Photovoltaic Modules with P-Type and N-Type Cells

Thallys Luan Bezerra Lima, Fernando Schuck de Oliveira, Mendelsson Rainer Macedo Neves, Diego Lucas de Carvalho Martinez and Tárcio André dos Santos Barros

Universidade Estadual de Campinas (UNICAMP)/ Laboratory of Energy and Photovoltaic Systems - Marcelo Villalva (LESF-MV), Campinas (Brazil)

Abstract

Potential-Induced Degradation (PID) affects the performance of photovoltaic modules, especially under high-voltage, high-humidity, and high-temperature conditions. This study evaluates the effects of PID on commercial modules with different cell technologies: p-type (PERC) and n-type (TOPCon). Three modules were subjected to two accelerated stress cycles, each lasting 96 hours, conducted at 85 °C and 85 % relative humidity under both positive and negative bias, in accordance with IEC 61215-2:2021 and IEC TS 62804-1:2015 standards. Electroluminescence (EL) images and I–V and P–V curves were used to monitor the progression of degradation in each sample. The results showed that the p-type module exhibited high PID susceptibility under negative bias, with intense darkening and a cumulative power loss of 14.6%. However, the n-type modules, generally considered more resistant, also experienced significant degradation under both polarities, with power losses of 12.3% under positive bias and 14.3% under negative bias. These findings demonstrate that despite the structural advantages of TOPCon cells, this technology remains susceptible to PID under continuous stress in both polarities. In large-scale photovoltaic systems, these losses can proportionally affect overall performance, significantly impacting the performance ratio (PR) and energy yield over the lifetime of the plant.

Keywords: potential-induced degradation, photovoltaic modules, p-type, n-type, electroluminescence, I–V curves.

1. Introduction

The installation of photovoltaic systems has grown significantly over the past decade in response to the global demand for renewable energy sources, both in Brazil and worldwide. Figure 1 shows the recent evolution of global photovoltaic installations, highlighting the rapid expansion of the technology (Masson et al., 2025). In Brazil, the scenario is equally remarkable: the installed capacity of centralized systems already exceeds 17 GW, while distributed generation, mainly composed of residential, commercial, and industrial systems, totals more than 39 GW, representing 23 % of the total capacity of the national electric grid (ABSOLAR, 2025).

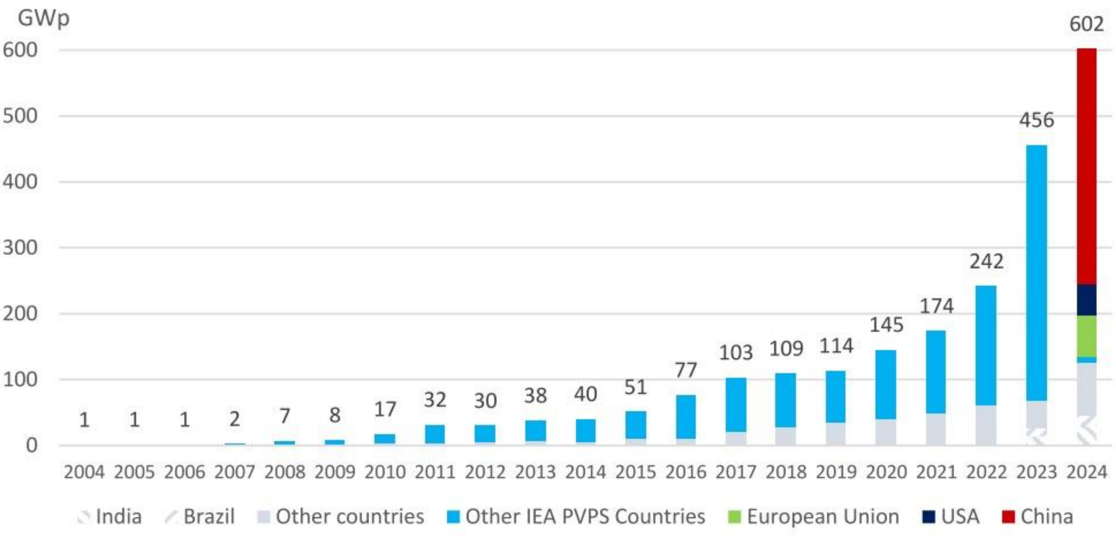

Figure 1: Annual evolution of photovoltaic installations worldwide (Adapted from Masson et al., 2025).

10.18086/swc.2025.03.06 Available at http://proceedings.ises.org

With the accelerated expansion of large-scale adoption, concerns have arisen regarding the reliability and durability of PV modules, especially in environments with high temperature and humidity. Among the main failure and degradation mechanisms observed in the field, potential-induced degradation (PID) stands out due to its direct impact on electrical performance loss. This phenomenon occurs when modules operate under high voltage relative to ground, creating a strong electric field between the cells and the grounded frame, which promotes ion migration through the encapsulant layers. This process affects the electrical performance of the cells, gradually reducing module power and efficiency and, in the long term, compromising its lifetime and the economic return of photovoltaic systems (Pingel et al., 2010; Luo et al., 2017; Aghaei et al., 2022).

With the evolution of cell architectures, technologies such as PERC (Passivated Emitter and Rear Cell) and TOPCon (Tunnel Oxide Passivated Contact) have become predominant in the photovoltaic market. The severity of PID is directly related to the cell structure and the materials used in module manufacturing. P-type cells, such as PERC, are more susceptible under negative bias (PID-s) due to the migration of sodium ions through the encapsulation and passivation layers, leading to the formation of electrical shunts and increased surface recombination (Gou et al., 2018; Huai et al., 2022). In contrast, n-type cells, such as TOPCon, exhibit greater resistance to PID under negative bias because of their advanced passivation structure. However, they can experience degradation under positive bias (PID-p), caused by the accumulation of positive charges in the dielectric layers, which hinders minority-carrier collection and reduces the device's electrical efficiency (Šlamberger et al., 2018; Carolus et al., 2019; Luo et al., 2020; Yamaguchi et al., 2018; Ohdaira et al., 2023).

Comparative studies show that the polarity of the applied voltage plays a decisive role in the manifestation of PID. P-type cells tend to degrade under negative voltage, while n-type cells may be affected under both polarities, depending on the passivation structure and materials used (Šlamberger et al., 2018; Luo et al., 2018).

Despite recent advances in understanding PID mechanisms, there is still a lack of comparative experimental studies involving modern commercial modules subjected to multiple stress cycles and different voltage polarities. Understanding how each technology responds under these conditions is important for improving the durability, performance, and long-term reliability of photovoltaic systems in operation.

In this context, this study comparatively investigates the effect of PID on commercial modules with p-type (PERC) and n-type (TOPCon) cells. Three modules were tested: one p-type subjected to negative bias (–1500 V), and two n-type modules, identical in brand and model, subjected to opposite polarities (+1500 V and –1500 V). Each sample was exposed to two 96-hour cycles at a temperature of 85 °C and 85 % relative humidity, following the test procedures defined in IEC 61215-2:2021 and IEC TS 62804-1:2015.

2. Potential-Induced Degradation (PID)

Potential-induced degradation (PID) is an electrochemical phenomenon that compromises the performance of photovoltaic modules when they operate under high voltages relative to the grounded structure, especially in environments with high temperature and humidity (Luo et al., 2017). In large-scale systems, where operating voltages often exceed 600 V, the electric field between the solar cells and the metallic frame promotes the migration of contaminant ions, such as sodium (Na^+), through the encapsulation and passivation layers. This migration reduces insulation resistance, generates leakage currents, and causes progressive power losses, ultimately compromising module reliability and lifetime (Pingel et al., 2010).

The phenomenon is generally classified into three main modes. The first is PID-s (shunting), which is associated with the formation of current-leakage paths due to Na^+ ion penetration into dielectric layers. The second is PID-p (polarization), characterized by the accumulation of positive charges in the front passivation layers, especially in n-type cells. Finally, PID-c (corrosion) results from electrochemical processes that degrade metallic contacts (Yamaguchi et al., 2018; Martinez-Loran et al., 2022).

In p-type cells, particularly those with PERC architectures, PID-s is the most common degradation mode. Under negative bias, Na^+ ions migrate from the front glass to the interface between silicon and silicon nitride (Si/SiNx), creating electrical shunts and reducing the open-circuit voltage (Voc) and fill factor (FF) (Gou et al., 2018). The severity of this process strongly depends on the chemical composition of the encapsulant and the quality of the passivation. In some cases, partial recovery can be achieved by applying reverse bias or through thermal treatment (Huai et al., 2022).

N-type cells, such as TOPCon, exhibit greater resistance to PID-s but are susceptible to PID-p, particularly under positive bias. In this mode, positive charges accumulate in the front passivation layer (SiNx), reducing the internal electric field and increasing minority-carrier recombination, which leads to reductions in both current and voltage (Ohdaira et al., 2023). Recent studies have also reported a second degradation phase, associated with a decrease in FF, attributed to Na^+ ion migration toward the p^+–n junction region (Komatsu et al., 2018). This degradation can be partially reversible through light exposure or the application of opposite bias (Wu et al., 2023).

The intensity of potential-induced degradation (PID) results from the interaction between intrinsic and extrinsic factors of the module. These factors can be grouped into four main levels: cell, module, system, and environment, as illustrated in Figure 2.

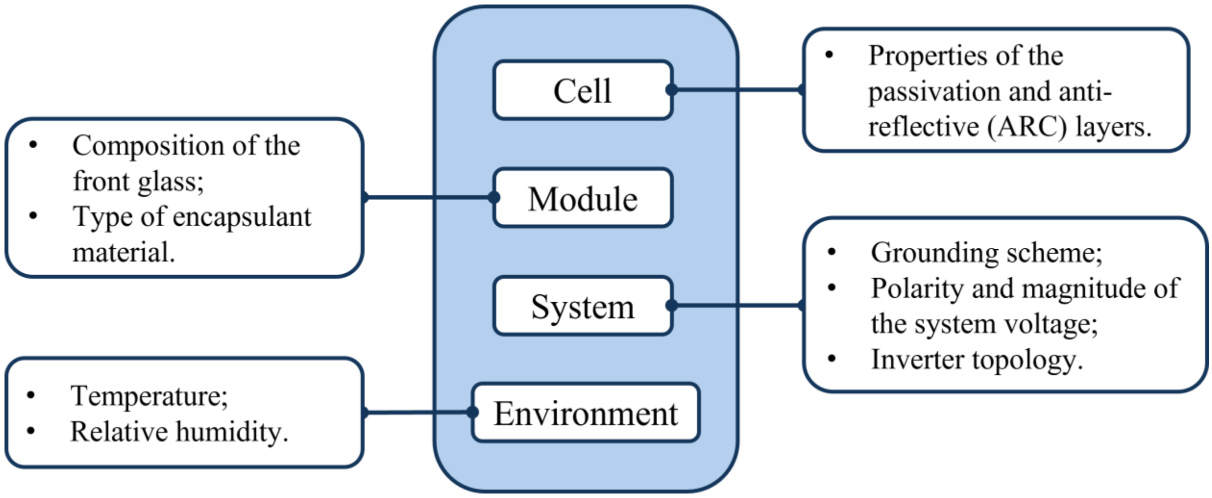

Figure 2: Main factors influencing the intensity of PID.

At the environmental level, conditions such as high temperature and relative humidity promote contaminant ion migration and intensify degradation mechanisms. At the system level, the inverter topology, grounding scheme, and the polarity and magnitude of the applied voltage determine the electric field established between the cells and the grounded frame, directly influencing the occurrence and severity of PID. At the module level, the sodium content of the front glass and the diffusion resistance of the encapsulant affect the rate of ion migration and the susceptibility to defect formation. Finally, at the cell level, characteristics such as doping type, passivation layers, and anti-reflective coatings determine both the manifestation and severity of degradation (Luo et al., 2017; Ohdaira et al., 2023; Komatsu et al., 2018).

Direct comparison between p-type and n-type technologies remains limited in studies involving commercial modules. Šlamberger et al. (2018) showed that n-type cells exhibit smaller power losses associated with PID, although polarization effects are still observed. Furthermore, recovery mechanisms and the influence of encapsulant materials differ between the two types, highlighting the need for comparative experimental investigations under controlled conditions.

This degradation manifests gradually during field operation. To evaluate and reproduce these effects under controlled conditions, the International Electrotechnical Commission (IEC) proposed standardized accelerated test procedures, described in IEC 61215-2:2021 and IEC TS 62804-1:2015. These standards define laboratory methods to assess the susceptibility and impact of PID in PV modules by simulating high-voltage, humidity, and temperature conditions that can occur in large-scale systems over time.

The most common accelerated test, known as Method A, subjects modules to 60 °C and 85 % relative humidity for 96 hours under the maximum system voltage specified by the manufacturer. To increase test severity, temperatures up to 85 °C may be used. Method B employs a conductive electrode (typically an aluminum foil) placed on the front glass, applying the same voltage for 168 hours at 25 °C, which allows the evaluation of polarization effects under less extreme thermal conditions (IEC 62804-1:2015).

3. Methodology

The methodology of this study was structured into five main stages: sample selection, initial characterization, thermo-electrical stress testing (accelerated PID cycles), post-stress characterization, and results analysis. The methodological flow followed in this work is presented in Figure 3, in accordance with IEC 61215-2:2021 and IEC TS 62804-1:2015 standards, which establish standardized procedures for qualification and potential-induced degradation (PID) susceptibility testing in photovoltaic modules.

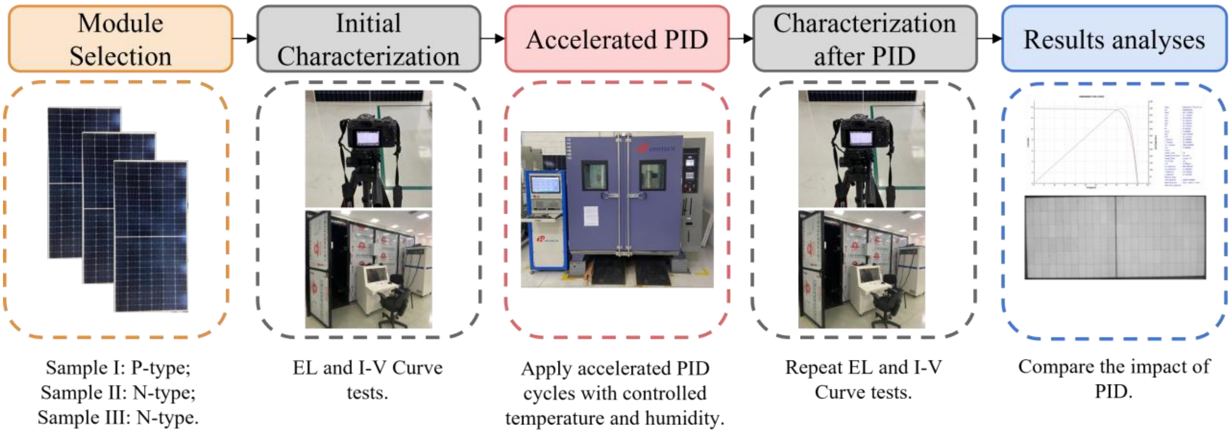

Figure 3: Methodological flow of the study.

In the first stage, three monofacial crystalline silicon modules available at the Laboratory of Energy and Photovoltaic Systems – Marcelo Villalva (LESF-MV), part of the Faculty of Electrical and Computer Engineering at UNICAMP, were selected. One module uses p-type cells with PERC technology, while the other two use n-type cells with TOPCon technology. The latter two modules are identical in brand, model, and nominal power, allowing a direct assessment of the effect of applied polarity during PID testing.

The p-type module was subjected to negative bias (–1500 V), which represents the most common PID occurrence scenario in field conditions. Conversely, the two n-type modules were subjected to opposite polarities: one under positive bias (+1500 V) and the other under negative bias (–1500 V), aiming to compare their behavior under different stress directions. The main characteristics of the samples and their respective test conditions are summarized in Table 1.

Table 1: Sample characteristics and PID test conditions.

Sample	Cell Type	Technology	Module Type	Nominal Power (STC)	Applied Bias
A	p-type	PERC	Monofacial	550 W	Negative (−1500V)
B	n-type	TOPCon	Monofacial	620 W	Positive (+1500V)
C	n-type	TOPCon	Monofacial	620 W	Negative (−1500V)

During the initial characterization, the modules were evaluated using current–voltage (I–V) curves and electroluminescence (EL) imaging to document their electrical and visual conditions before testing. The I–V curves were measured using a class A+A+A+ solar simulator (GIV-20A2616, GSOLA®), which enables the acquisition of the characteristic curve of each module and allows comparison of electrical variations after degradation cycles.The EL images were captured in a dark environment using a Canon EOS RP camera equipped with a PVvision EL-Lens, enabling the observation of darkened regions and cell defects after exposure to stress conditions.

In the accelerated PID stress phase, the modules were subjected to two degradation cycles inside a HOTOTECH HTPV-16 climatic chamber (Damp Heat Testing Machine), capable of simulating critical environmental conditions that promote PID. Each cycle lasted 96 hours, with a temperature of 85 °C and relative humidity of 85%. During this period, a voltage of ±1500 V was applied according to the cell type and experimental objective. The voltage was applied between the module terminals, which were kept short-circuited, and the metallic frame, which was grounded. This configuration simulates the potential difference experienced by modules in grid-connected PV systems, thereby intensifying PID effects in a controlled manner, as recommended by IEC TS 62804-1:2015. Figure 4 presents an illustrative diagram of the electrical configuration used to apply the bias voltage during the test.

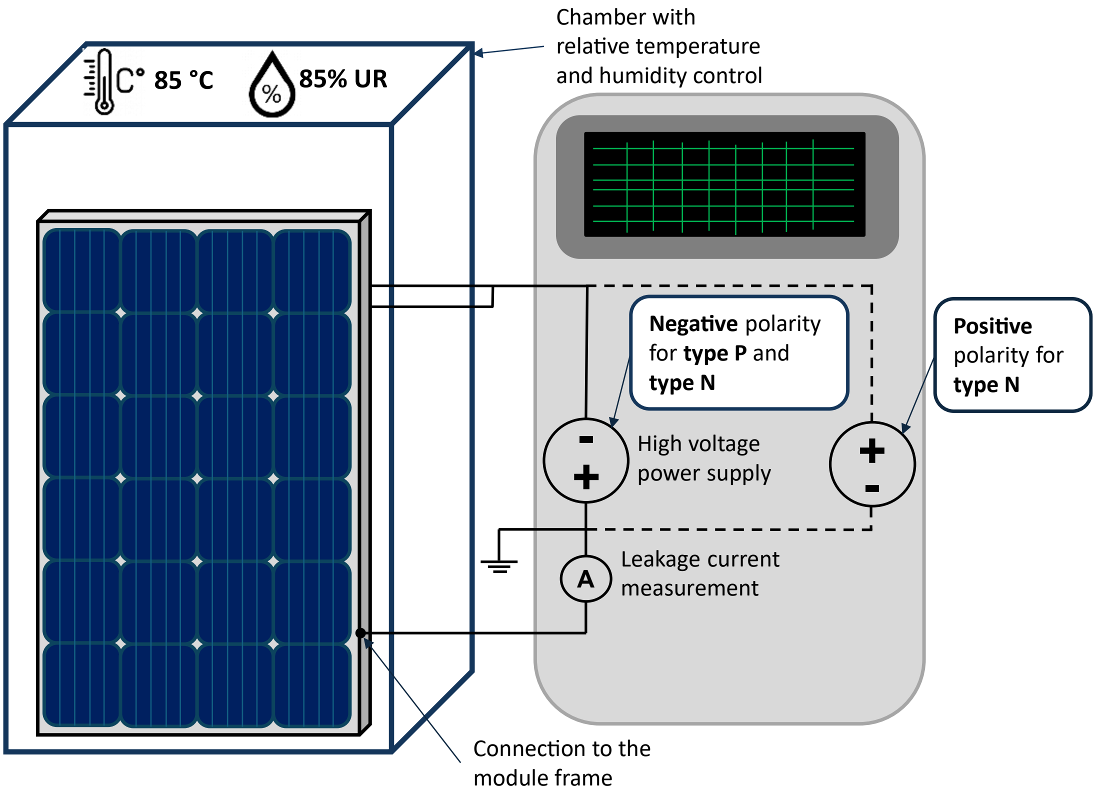

Figure 4: Experimental setup and electrical configuration for the accelerated PID test.

After each stress cycle, the characterization procedures were repeated. The new I–V curves and EL images allowed us to monitor the evolution of degradation throughout the cycles. By comparing data obtained before and after stress exposure, it was possible to calculate relative performance losses and identify visible structural changes in the cells, such as the appearance of new affected regions.

Finally, the results were analyzed both individually and comparatively. The objective was to identify the intensity and location of PID-induced damage in each module and to understand the impact of stress polarity on n-type cells. The analysis also enabled evaluation of behavioral differences between p-type and n-type technologies, as well as the progression of degradation between the first and second cycles. This approach provided a comprehensive understanding of the mechanisms of potential-induced degradation under different experimental conditions, contributing valuable insights toward improving the reliability of modern commercial PV modules.

4. Results and Discussion

The following results present the analysis of PID effects on three photovoltaic modules with different cell technologies and voltage polarities. The discussion covers electroluminescence images and I–V and P–V curves obtained before and after two accelerated stress cycles. This approach allows comparison of the degradation severity between p-type and n-type cells under different bias conditions.

The EL images shown in Figure 5 illustrate the evolution of PID-related degradation over two stress cycles in the p-type (PERC) module subjected to negative bias. In the initial condition, the luminous emission is homogeneous, indicating good cell uniformity and the absence of significant structural defects. After the first cycle, darkened areas appear, distributed non-uniformly and mainly concentrated along the module edges. These regions indicate increased carrier recombination and the formation of leakage paths, which are typical manifestations of PID in p-type cells. After the second cycle, the darkened regions expand and intensify, revealing the continuous progression of degradation under thermo-electrical stress.

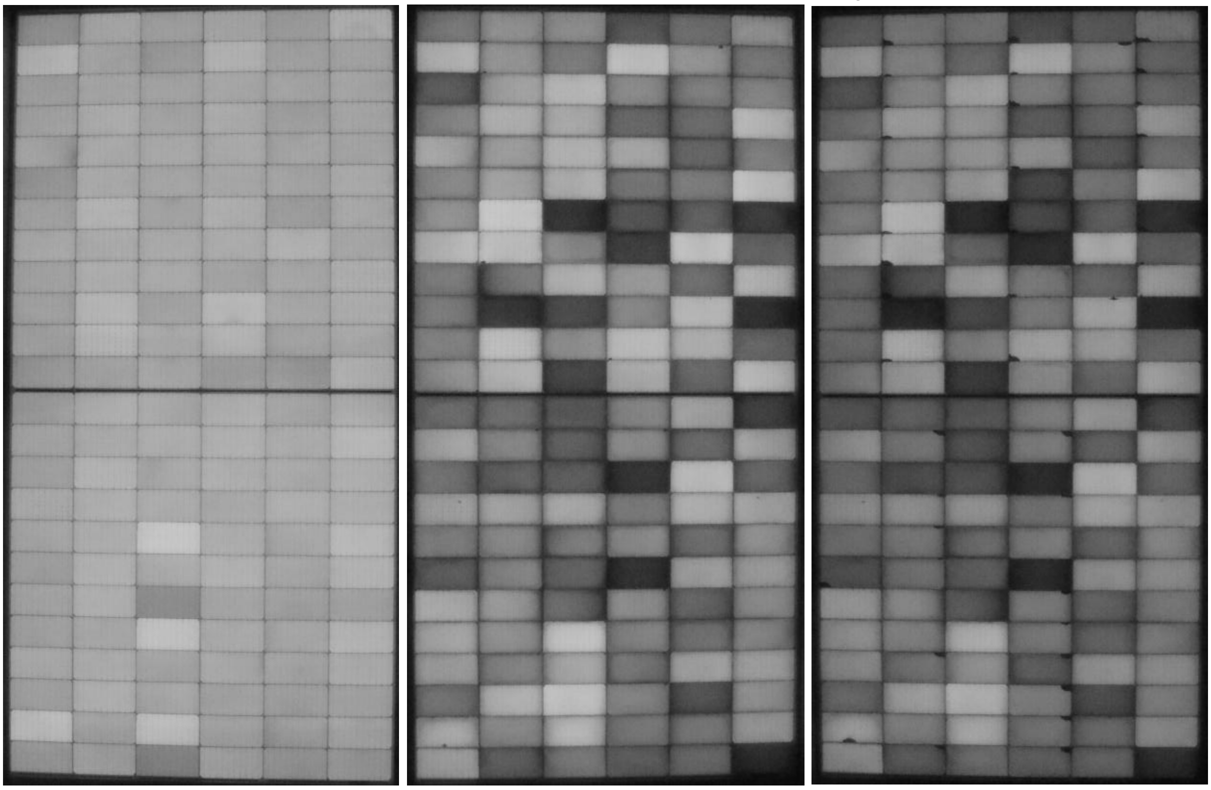

(a) (b) (c)

Figure 5: EL images of the p-type module: (a) initial, (b) after one cycle, and (c) after two cycles of accelerated PID under negative potential.

The I–V and P–V curves in Figure 6 confirm the degradation trends previously observed in the EL analysis. A progressive reduction in open-circuit voltage (Voc) and short-circuit current (Isc) indicates a deterioration of the module's electrical performance. The maximum power (Pmax) decreased from 514 W in the initial state to 447 W after the first cycle and 439 W after the second. These losses are consistent with Na^{+} ion migration and the formation of electrical shunts, characteristic of the PID-s mechanism.

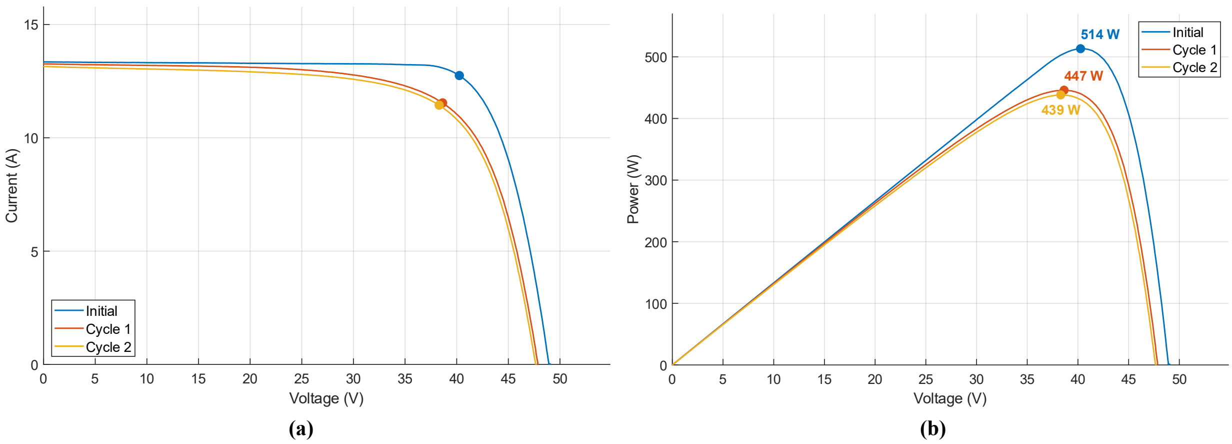

(a) (b)

Figure 6: I–V (a) and P–V (b) curves of the p-type module along two accelerated PID cycles under negative potential.

The EL images in Figure 7 depict the progression of PID-related degradation in the n-type (TOPCon) module under positive bias. Initially, the module shows uniform emission over the entire active area, with no significant structural defects. After the first stress cycle, darkened regions become visible near the edges, indicating the onset of local degradation. This effect intensifies after the second cycle, with expanded affected areas and diminished emission across several cells, evidencing the accumulation of positive charges in the dielectric layer.

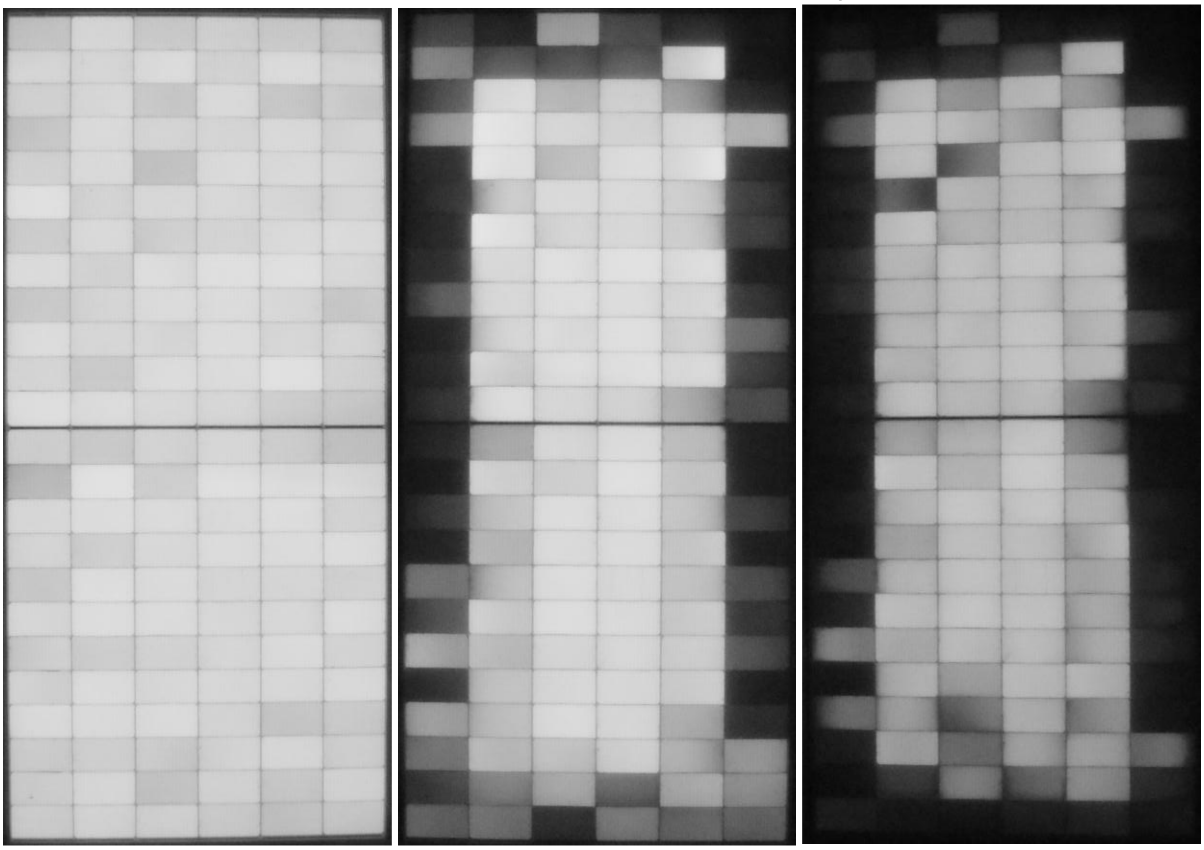

(a) (b) (c)

Figure 7: EL images of the n-type module: (a) initial, (b) after one cycle, and (c) after two cycles of accelerated PID under positive potential.

The electrical behavior, shown in Figure 8, mirrors the visual degradation. Both Isc and Voc decrease progressively, while the maximum power drops from 625 W to 573 W after the first cycle and to 548 W after the second. Although n-type cells initially exhibit higher resistance to PID, the results confirm that continuous positive bias can significantly impact their performance.

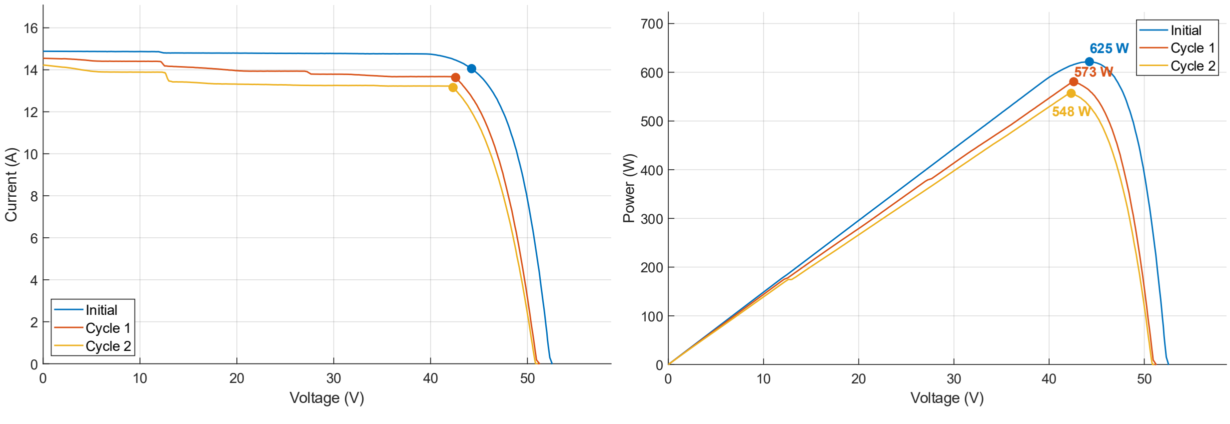

(a) (b)

Figure 8: I–V (a) and P–V (b) curves of the n-type module along two accelerated PID cycles under positive potential.

The EL images in Figure 9 show the cumulative degradation effects on the n-type (TOPCon) module tested under negative bias. The initial state exhibits uniform emission, but after the first stress cycle, darkened zones appear along the upper and lower edges. Following the second cycle, the darkening becomes more extensive and diffuse, particularly in the central and lower regions, confirming that even n-type cells can suffer significant degradation when exposed to a continuous negative potential.

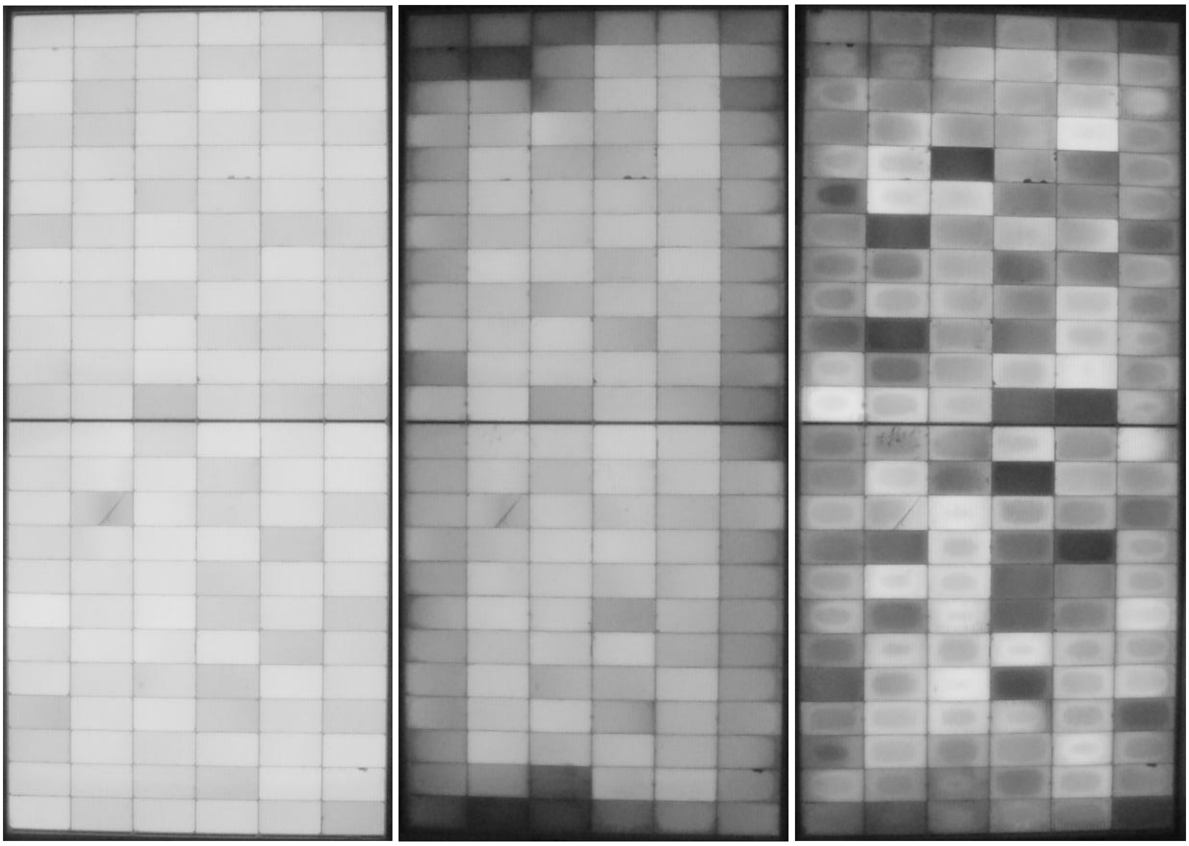

(a) (b) (c)

Figure 9: EL images of the n-type module: (a) initial, (b) after one cycle, and (c) after two cycles of accelerated PID under negative potential.

The electrical results presented in Figure 10 complement the EL analysis. A continuous decrease in both Isc and Voc is observed, along with a marked reduction in maximum power from 622 W initially to 596 W after the first cycle and 533 W after the second. These findings demonstrate that prolonged negative bias can induce substantial electrical and structural degradation even in modules based on n-type technology.

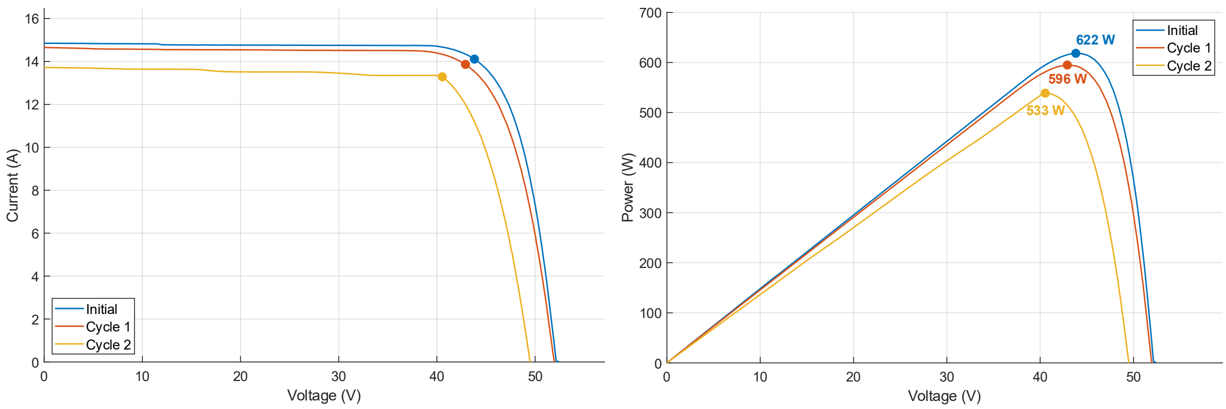

(a) (b)

Figure 10: I–V (a) and P–V (b) curves of the n-type module along two accelerated PID cycles under negative potential.

Table 2 consolidates the main electrical parameters measured for the modules before and after two degradation cycles. It can be observed that Sample A (p-type) exhibited the most significant P_{max} loss, decreasing from 514 W to 439 W, accompanied by reductions in V_{oc}, I_{sc}, and shunt resistance (R_{sh}). This behavior is characteristic of the PID-s degradation mode, often associated with Na^+ ion migration and the formation of electrical leakage paths in p-type cells. For Samples B and C (n-type), degradation effects were also noticeable. Sample B, under positive bias, showed a decrease in P_{max} from 625 W to 548 W, while Sample C, under negative bias, exhibited a similar reduction from 622 W to 533 W.

Table 2: Electrical parameters of PV modules before and after accelerated PID cycles.

Sample	Cycle	P_{max} (W)	V_{oc} (V)	I_{sc} (A)	V_{mp} (V)	I_{mp} (A)	R_{sh} (Ω)
A (p-type)	Initial	514	48.95	13.34	40.42	13.35	285.24
	Cycle 1	447	47.87	13.26	38.65	11.55	148.79
	Cycle 2	439	47.65	13.14	38.43	11.42	88.24
B (n-type)	Initial	625	52.45	14.88	44.27	14.12	569.80
	Cycle 1	573	51.08	14.56	42.76	13.40	48.14
	Cycle 2	548	50.86	14.21	42.28	12.97	21.66
C (n-type)	Initial	622	52.21	14.85	44.08	14.10	342.77
	Cycle 1	596	51.97	14.65	43.10	13.84	98.42
	Cycle 2	533	49.50	13.73	40.92	13.03	119.98

Table 3 summarizes the relative losses of maximum power over the two test cycles. The p-type module showed the highest loss after the first cycle, with a 13.1% reduction in Pmax. In contrast, the n-type modules degraded more gradually, reaching cumulative losses of 12.3% and 14.3% only after the second cycle. This behavior suggests that n-type cells have greater initial resistance. Still, their passivation layers can be compromised under prolonged stress, regardless of whether the applied bias is positive or negative.

Table 3: Relative loss of maximum power (P_{max}) for each sample under PID conditions.

Sample	Potential	Maximum Power (W)			Relative Loss (%)	
		Initial	Cycle 1	Cycle 2	After Cycle 1	After Cycle 2
A (p-type)	Negativo (−1500V)	514	447	439	13.1	14.6
B (n-type)	Positivo (+1500V)	625	573	548	8.3	12.3
C (n-type)	Negativo (−1500V)	622	596	533	4.2	14.3

5. Conclusions

This study presented an experimental analysis of potential-induced degradation (PID) effects in commercial photovoltaic modules with different cell technologies, p-type (PERC) and n-type (TOPCon), subjected to two accelerated stress cycles under both positive and negative bias. Monitoring degradation through electroluminescence (EL) imaging and I–V and P–V curve analysis enabled a comparative evaluation of power loss in each technology.

The results showed that the p-type module exhibited high sensitivity to PID under negative bias, with a 14.6% reduction in P_{max} after the second cycle. The EL images revealed darkened regions distributed along the module, associated with shunt formation and loss of surface passivation, which are typical characteristics of the PID-s mode.

However, one of the most relevant findings of this study was that n-type modules, often regarded by manufacturers as more resistant to PID, also exhibited significant degradation under both polarities. The sample subjected to positive bias lost 12.3% of P_{max}, while the one under negative bias showed a 14.3% loss after the second cycle. EL images revealed noticeable darkening, and the electrical curves confirmed declines in V_{oc}, I_{sc}, and R_{sh}, indicating passivation degradation and increased minority-carrier recombination.

These results demonstrate that, despite the structural advantages of TOPCon cells, such as improved passivation and opposite doping on the rear side, the technology remains susceptible to PID, especially under prolonged stress conditions. The degradation observed under both polarities suggests that the assumed PID immunity of n-type cells should be reconsidered, given the varying operating conditions and system topologies.

Furthermore, the power losses observed in the tested modules represent proportional linear performance losses in large-scale photovoltaic plants. When combined with other degradation mechanisms, these effects can become substantial, reducing both the performance ratio (PR) and the overall energy yield throughout the plant's lifetime. Such findings highlight the importance of preventive mitigation strategies and ongoing research aimed at improving the durability and long-term reliability of emerging photovoltaic technologies.

6. Acknowledgments

This study was financed by TotalEnergies through the R&D incentive program of the Brazilian National Agency of Petroleum, Natural Gas and Biofuels (ANP) in partnership with CEPETRO and FEEC at UNICAMP.

7. References

ABSOLAR, 2025. Energia Solar no Brasil: Infográfico ABSOLAR. Associação Brasileira de Energia Solar Fotovoltaica. Disponível em: https://www.absolar.org.br/mercado/infografico/. Acesso em: 16 jul. 2025.

Aghaei, M., Fairbrother, A., Gok, A., Ahmad, S., Kazim, S., Lobato, K., Oreski, G., Reinders, A., Schmitz, J., Theelen, M., Yilmaz, P., Kettle, J., 2022. Review of degradation and failure phenomena in photovoltaic modules. Renewable and Sustainable Energy Reviews 159, 112160. https://doi.org/10.1016/j.rser.2022.112160.

Carolus, J., Tsanakas, I.A., van der Heide, A., Voroshazi, E., De Ceuninck, W., Daenen, M., 2019. Physics of potential-induced degradation in bifacial p-PERC solar cells. Solar Energy Materials and Solar Cells 200, 109950. https://doi.org/10.1016/j.solmat.2019.109950.

Gou, J., Li, Y., Cui, Y., Zhou, Q., 2018. Effects of diffusion process on potential-induced degradation of silicon solar cells. Journal of Applied Biomaterials & Functional Materials 16(3), 185–192. https://doi.org/10.1177/2280800017753946.

Huai, J., Takada, K., Tsuruta, K., Tokumasu, H., Takano, I., 2022. Recovery of potential-induced degraded p-type multicrystalline Si PV modules by application of a reverse DC bias. Japanese Journal of Applied Physics 61, 046503. https://doi.org/10.35848/1347-4065/ac52d5.

International Electrotechnical Commission (IEC), 2015. Photovoltaic (PV) Modules – Test Methods for the Detection of Potential-Induced Degradation. IEC 62804-1:2015, United Kingdom, September 2015.

International Electrotechnical Commission (IEC), 2021. Terrestrial Photovoltaic (PV) Modules – Design Qualification and Type Approval – Part 2: Test Procedures. IEC 61215-2:2021, Brussels, Belgium, April 2021.

Komatsu, Y., Yamaguchi, H., Ohdaira, K., 2018. Multistage performance deterioration in n-type crystalline silicon solar cells due to potential-induced degradation. Microelectronics Reliability 84, 127–133. https://doi.org/10.1016/j.microrel.2018.03.018.

Luo, W., Chen, T., Zhang, Y., Khoo, Y.S., Lin, Q., Yao, Y., Aberle, A.G., 2018. Investigation of potential-induced degradation in n-PERT bifacial silicon photovoltaic modules with a glass/glass structure. IEEE Journal of Photovoltaics 8(1), 16–22. https://doi.org/10.1109/JPHOTOV.2017.2762587.

Luo, W., Khoo, Y.S., Hacke, P., Naumann, V., Lausch, D., Harvey, S.P., Singh, J.P., Chai, J., Wang, Y., Aberle, A.G., 2017. Potential-induced degradation in photovoltaic modules: a critical review. Energy & Environmental Science 10(1), 43–68. https://doi.org/10.1039/C6EE02271E.

Martinez-Loran, E., Gastrow, G. van der, Alonso-Abella, M., 2022. Finite element simulation of potential-induced degradation kinetics in p-type silicon solar modules. IEEE Journal of Photovoltaics 12(1), 45–52. https://doi.org/10.1109/JPHOTOV.2021.3123870.

Masson, G., Van Rechem, A., de l'Epine, M., Jäger-Waldau, A., 2025. Snapshot of Global PV Markets 2025. International Energy Agency – Photovoltaic Power Systems Programme (IEA PVPS).

Ohdaira, K., Komatsu, Y., Yamaguchi, H., 2023. Second-stage potential-induced degradation of n-type front-emitter crystalline silicon photovoltaic modules and its recovery. Japanese Journal of Applied Physics 62, 086601. https://doi.org/10.35848/1347-4065/accb60.

Pingel, S., Frank, O., Winkler, M., Oryan, S., Geipel, T., Hoehne, H., Berghold, J., 2010. Potential-induced degradation of solar cells and panels. In: Proceedings of the 35th IEEE Photovoltaic Specialists Conference

(PVSC), Honolulu, USA, pp. 2817–2822. https://doi.org/10.1109/PVSC.2010.5616823.

Šlamberger, J., Topič, M., Jerič, T., 2018. Comparison of potential-induced degradation (PID) of n-type and p-type silicon solar cells. Energy 161, 266–276. https://doi.org/10.1016/j.energy.2018.07.118.

Wu, M., Tu, Z., Chen, D., Deng, J., Li, Y., Li, L., 2023. Delay of the potential-induced degradation of n-type crystalline silicon PV modules by the prior application of reverse bias. Japanese Journal of Applied Physics 63(2), 02SP06. https://doi.org/10.35848/1347-4065/ad02a6.

Yamaguchi, H., Nakamura, K., Tsuruta, K., Tokumasu, H., Takano, I., 2018. Rapid progression and subsequent saturation of potential-induced degradation in n-type bifacial crystalline silicon solar cells. Japanese Journal of Applied Physics 57, 122301. https://doi.org/10.7567/JJAP.57.122301.